



## RESEARCH ARTICLE

# Design of a circular dual-loop antenna for a GPS array element using an extended cavity structure

Jun Hur<sup>1</sup> | Gangil Byun<sup>2</sup>  |  
JongSung Kim<sup>3</sup> | Misuk Kim<sup>3</sup> |  
Jinwon Ko<sup>4</sup> | Hosung Choo<sup>1</sup> 

<sup>1</sup>School of Electronic and Electrical Engineering, Hongik University, Seoul, Korea

<sup>2</sup>School of Electrical Computer Engineering, Ulsan National Institute of Science and Technology, Ulsan, Korea

<sup>3</sup>Department of Alternative Navigation Division, NAVCOURS Co., Ltd., Daejeon, South Korea

<sup>4</sup>Center of the AESA RADAR R&D, Hanwha Systems, Seongnam, Gyeonggi, South Korea

## Correspondence

Hosung Choo, Hongik University, 94 Wausan-Ro, Mapo-Ku, Seoul 04066, Korea.

Email: hschoo@hongik.ac.kr

## Funding information

Hanwha Systems; Navcours Co., Ltd.

## Abstract

This article proposes a circular dual-loop antenna for a very small Global Positioning System array with an extended cavity structure. The antenna element consists of lower and upper circular loops printed on a high-dielectric ceramic substrate and an extended cavity structure above the ground plane to improve the isolation characteristic. To demonstrate the suitability of the proposed antenna, antenna characteristics are measured in a full-anechoic chamber, and its performances such as bore-sight gain, mutual coupling, and near-field as a function of extended cavity height are analyzed. The results confirm that the proposed antenna structure can minimize the gain degradation by improving the isolation characteristic and is therefore suitable for use in very small arrays.

## KEYWORDS

antenna array, cavity antenna, GPS antenna, microstrip loop antenna

## 1 | INTRODUCTION

Antenna arrays are widely used to minimize interference caused by jamming signals or multipath channel environments in the Global Positioning System (GPS). The array antenna has a mutual coupling effect between adjacent antenna elements, and this effect is enlarged when the number of array elements is increased within a narrow mounting space. The improvement of isolation characteristic between the array elements is essential because the mutual coupling results in the reduced bore-sight gain and pattern distortion, especially in extremely small GPS arrays. The mutual coupling can be reduced by inserting an additional structure between antenna elements.<sup>1–3</sup> However, this approach has disadvantages, including increased manufacturing costs and complexity. Thus, some previous studies have focused on minimizing the antenna size by using lumped elements,<sup>4</sup> metamaterial substrates,<sup>5,6</sup> and slots in antenna radiators<sup>7</sup> to increase the physical separation distance between the array elements for isolation improvement. However, such studies require additional design parameters and lack an intensive consideration of mutual coupling caused by leakage fields from antenna elements in a very small array. Therefore, in-depth research of this issue is needed to develop effective methods to improve the isolation characteristic without increasing fabrication costs and design complexity.

In this article, we propose a design of a circular dual-loop antenna with an extended cavity that improves isolation by substantially reducing the leakage field. The proposed cavity structure helps to avoid significant gain reduction caused by the mutual coupling effect between the array elements and miniaturizes the antenna aperture size by maximizing the effective dielectric constant of the substrate. The proposed antenna is composed of a lower circular feed loop and an upper circular radiating loop that are printed on a high-dielectric ceramic substrate. The cavity structure, which can improve the isolation characteristic, is expanded above the ground plane to surround the entire lateral surface of the ceramic substrate. The lower feed loop is fed by two ports of a hybrid chip coupler (XC1400P-03S from Anaren) for circular polarization, and the upper loop is then magnetically coupled to the lower loop for achievement of the frequency-insensitive behavior.<sup>8</sup> We observe the antenna characteristics according to the height of an extended cavity structure to verify the improvement of isolation and the principle on antenna miniaturization. The results confirm that the proposed antenna can avoid the gain degradation by achieving isolation enhancement with the reduced

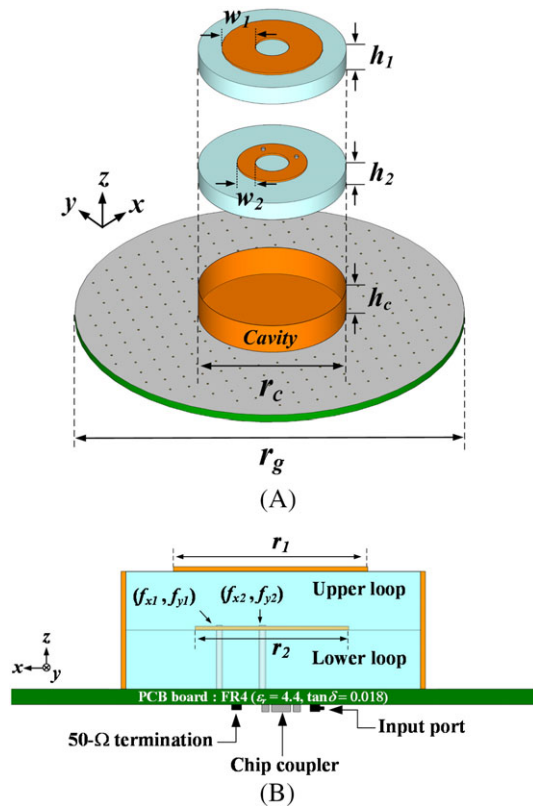


**FIGURE 1** Geometry of the proposed antenna. A, Top view. B, Side view [Colour figure can be viewed at [wileyonlinelibrary.com](https://onlinelibrary.wiley.com)]

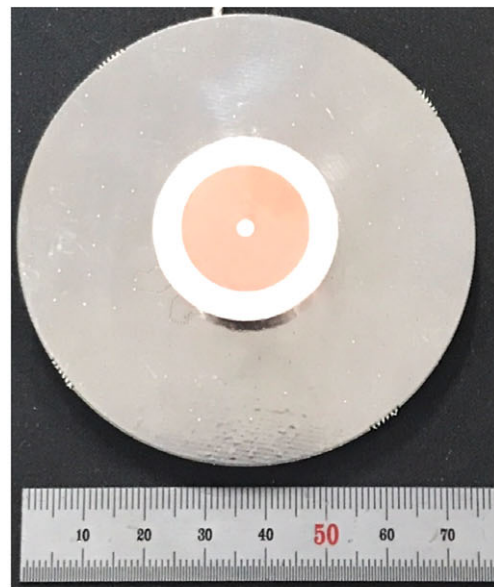
leakage field strength and miniaturized antenna size, and is therefore suitable for use in very small arrays.

## 2 | PROPOSED ANTENNA DESIGN AND MEASUREMENT

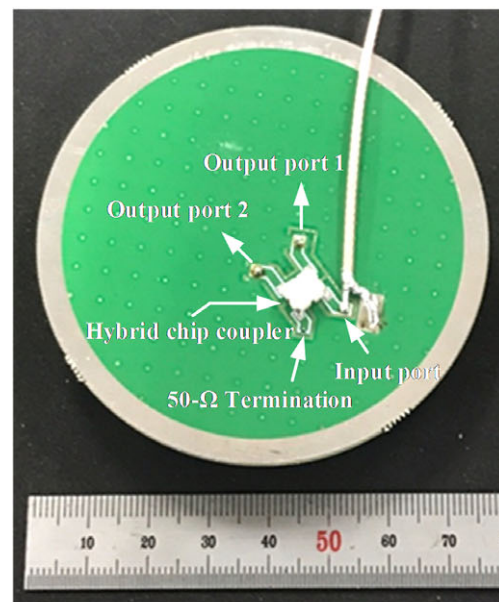
Figure 1 shows the geometry of the proposed GPS antenna element. The antenna consists of upper and lower circular loops printed on a high-dielectric ceramic substrate ( $\epsilon_r = 20$ ,  $\tan \delta = 0.004$ ) with thicknesses of  $h_1$  and  $h_2$ , respectively. The upper and lower circular loops are designed with diameters of  $r_1$  and  $r_2$ , and widths of  $w_1$  and  $w_2$ . The lower feed loop is directly connected to two ports of a hybrid chip coupler, denoted as  $(f_{x1}, f_{y1})$  and  $(f_{x2}, f_{y2})$  for circular polarization (CP) properties. The upper loop is electromagnetically coupled to the lower loop for low reactance variations, resulting in broadband operation.<sup>8</sup> The extended cavity structure resides above the ground plane and surrounds the entire lateral surface of the ceramic substrate. This extended cavity structure can reduce the leakage field from the antenna substrate and miniaturize the antenna size by increasing the effective permittivity of the substrate. The detailed design parameters are optimized by a genetic algorithm<sup>9</sup> and listed in Table 1. As can be seen, the extended

**TABLE 1** Optimized values of the proposed array

Parameter	$w_1$	$w_2$	$h_1$	$h_2$	$h_c$	$r_c$	$r_g$	$r_1$	$r_2$	$(f_{x1}, f_{y1})$	$(f_{x2}, f_{y2})$
Value (mm)	8.8	5.7	4	4	8	32	76	20.8	15	(5.9, 0)	(0, 5.9)



(A)

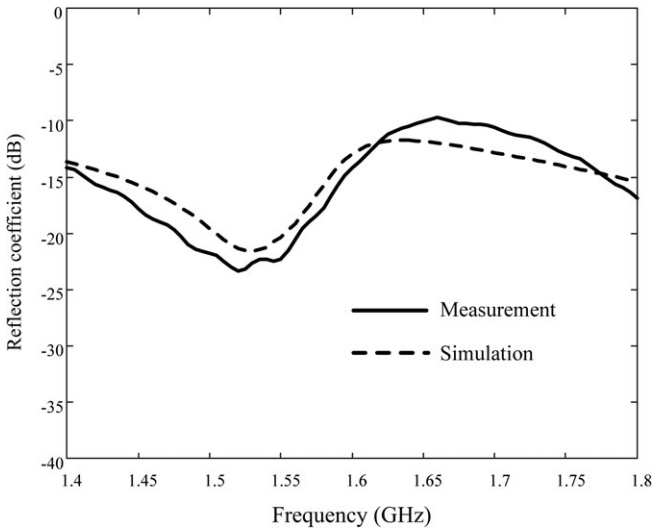


(B)

**FIGURE 2** Photographs of the fabricated antenna. A, Top view. B, Bottom view [Colour figure can be viewed at [wileyonlinelibrary.com](https://onlinelibrary.wiley.com)]

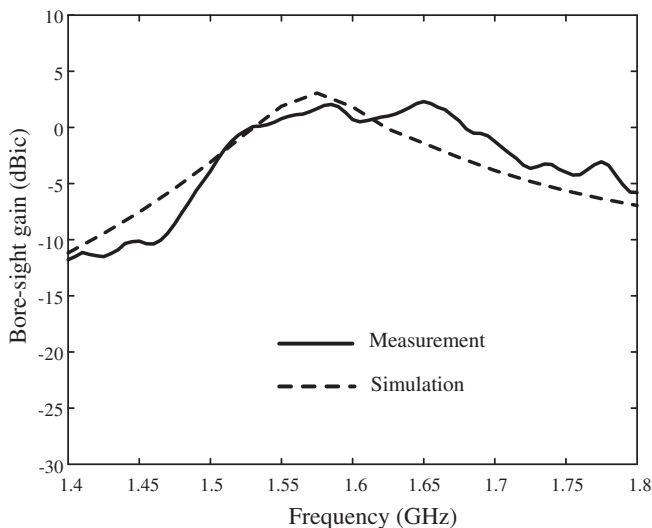
cavity that has a height of 8 mm covering the entire dielectric substrate, can improve the isolation characteristic by reducing the leakage field from the antenna.

Figure 2A shows a photograph of the proposed antenna printed on the ceramic substrate, and Figure 2B presents a printed circuit board that includes the hybrid chip coupler, coplanar waveguides, and a 50- $\Omega$  termination chip for a quadratic phase excitation. The antenna characteristics, such as the reflection coefficients, bore-sight gain, axial ratio (AR), and



**FIGURE 3** Reflection coefficient of the proposed antenna

radiation patterns, are measured in a full anechoic chamber. The measured and simulated reflection coefficient of the antenna as a function of the frequency is shown in Figure 3. To obtain the simulated reflection coefficients, we calculated the scattering matrix of the 2-port antenna by using the FEKO EM simulator<sup>10</sup> and is connected to two output ports in the 4-port network of the hybrid chip coupler in Ansys Designer.<sup>11</sup> The dashed line indicates the simulated values, and the solid line represents the measured data. Both results show good agreement with the measured value of  $-18.43$  dB at 1.575 GHz and  $-16.58$  dB of the simulated value. The reflection coefficients are less than  $-10$  dB in a wide frequency band from 1.4 to 1.8 GHz. This broadband impedance matching performance is obtained from the low reactance variations due to the coupled feeding between the loops and is also caused by the hybrid chip coupler characteristic which matched to the termination load of  $50 \Omega$  in a circuit of the component. Figure 4 shows the measured bore-sight gain compared with the simulated data. The simulated and measured values are 3.0 and 1.7 dBic at



**FIGURE 4** Bore-sight gain of the proposed antenna

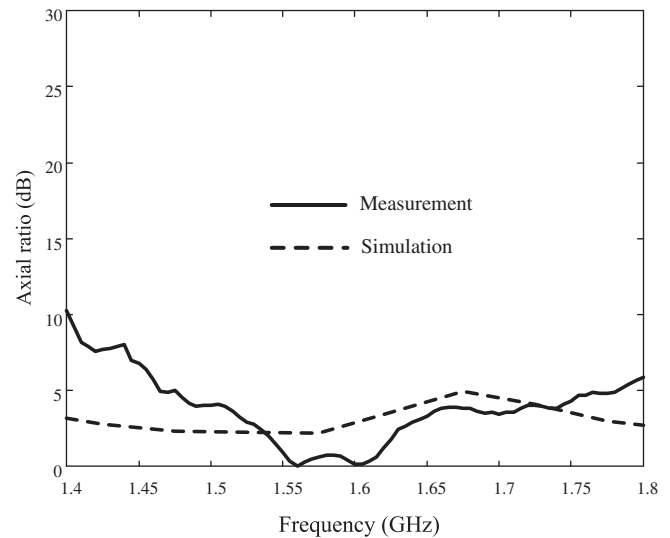
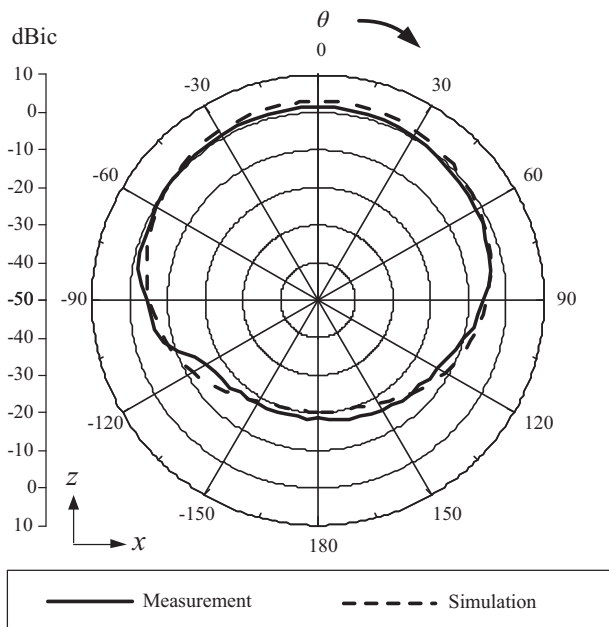


**FIGURE 5** Axial ratio of the proposed antenna

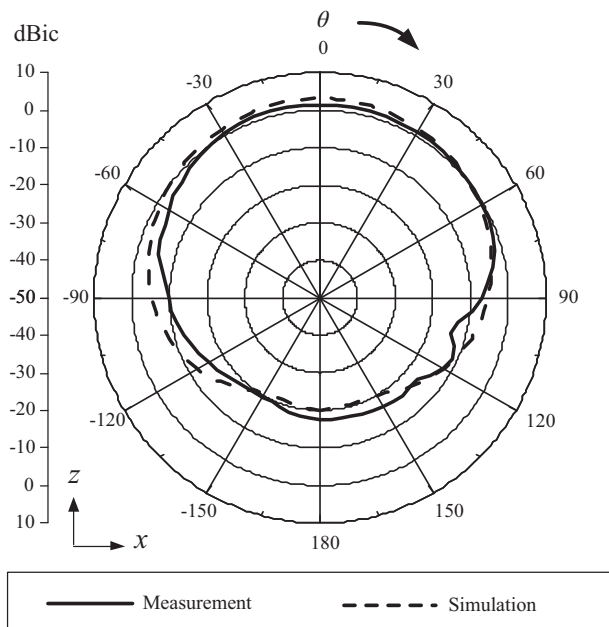
1.575 GHz and are greater than 0 dBic from 1.53 to 1.62 GHz. Figure 5 provides an AR of the antenna in the bore-sight direction. To calculate the measured ARs, a linearly polarized standard horn antenna is rotated for vertical and horizontal polarizations, and the received field magnitudes are used to calculate the ratio of the major and minor axes in the polarization ellipse.<sup>12</sup> The proposed antenna has a simulated AR value of 2.2 dB (1.575 GHz), and the measured value is 0.9 dB (1.575 GHz). The AR values are maintained below 3 dB in a wide frequency range, implying that the antenna can avoid a significant right-hand circular polarization (RHCP) gain reduction caused by the distorted polarization properties in a small GPS array. The radiation patterns of the antenna in the  $xz$ -planes and  $zy$ -planes at 1.575 GHz are shown in Figure 6. The measured half-power beamwidths at 1.575 GHz are  $140^\circ$  in the  $xz$ -plane and  $115^\circ$  in the  $zy$ -plane. As can be seen, the proposed antenna does not have any severe pattern distortion in the upper hemisphere.

### 3 | PARAMETRIC STUDY AND ANALYSIS

To verify the effectiveness of the extended cavity structure, we observe the bore-sight gain according to the extended cavity height ( $h_c$ ), as shown in Figure 7. The resonant frequency without an extended cavity ( $h_c = 0$  mm), indicated by the dotted line, is 1.65 GHz, and the resonance shifts to 1.6 GHz when the  $h_c = 4$  mm (dashed line). The solid line represents the proposed antenna with an extended cavity surrounding the entire lateral surface of the ceramic substrate ( $h_c = 8$  mm), in which the resonance frequency is 1.575 GHz. This phenomenon of resonant frequency shift according to the height of the extended cavity demonstrates that the proposed extended cavity structure reduces the antenna size by maximizing the effective permittivity of the



(A)



(B)

**FIGURE 6** Radiation patterns of the proposed antenna. A,  $xz$ -plane. B,  $zy$ -plane

substrate. Figure 8 presents the average magnetic field strengths at the resonance frequency of each antenna with different cavity heights ( $y = 0$  mm,  $0$  mm  $\leq z \leq 8$  mm). The value inside the substrate ( $x \leq 15$  mm) of the proposed extended cavity antenna, indicated by the solid line, is stronger than other antennas. For example, the strength at 15 mm is increased from 17.5 to 21.5 dBA/m by increasing the extended cavity height. It can be seen that the proposed extended cavity confines near fields within the cavity area to increase the effective permittivity of the dielectric. The H-field strength of the proposed antenna ( $h_c = 8$  mm) is rapidly reduced from the location of the extended cavity

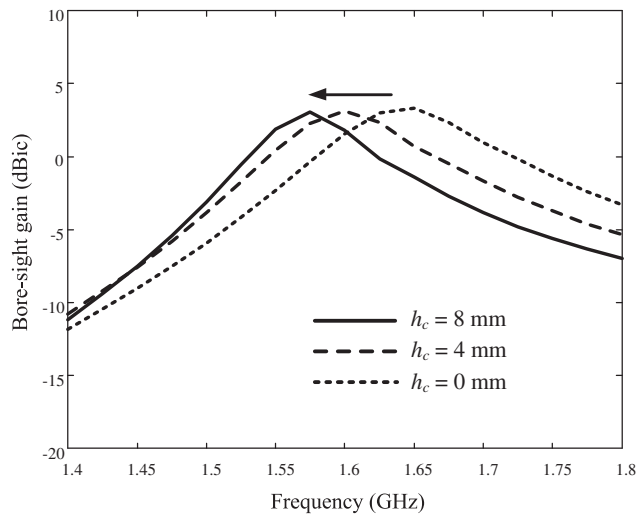
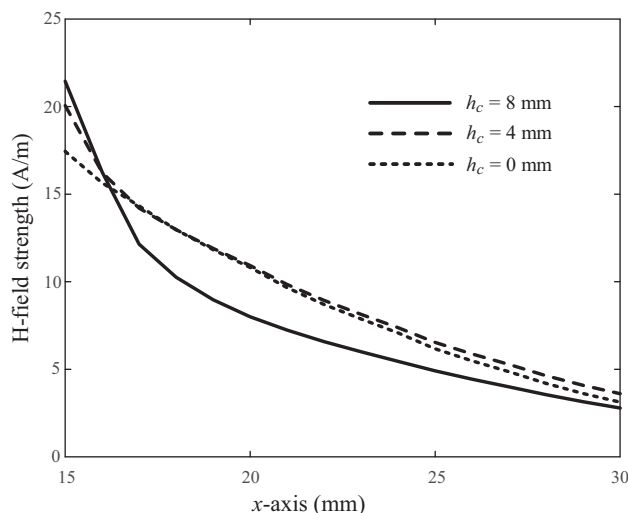


**FIGURE 7** Bore-sight gains according to the  $h_c$

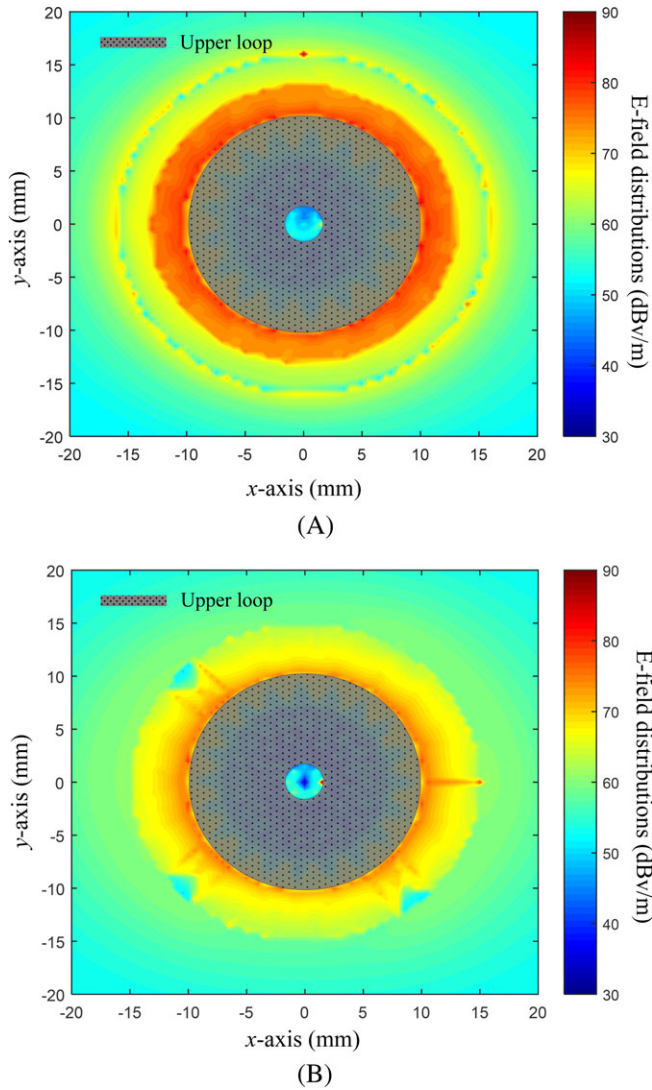
( $x = 15$  mm) compared to lower cavity heights (or less extended cavity structures). This leakage field reduction can lead to isolation improvement between the adjacent array elements in an extremely small GPS antenna array.

Figure 9A,B shows electric field distributions of the antennas with and without an extended cavity at each resonance frequency with and without cavity (1.575 and 1.65 GHz). The electric fields of the antenna with an extended cavity are more confined around the loop patch than the antenna without a cavity structure. The magnetic field distributions of the antennas with and without cavity presented in Figure 10A,B. The proposed antenna has a weak leakage field strength from the antenna substrate compared with the antenna without cavity, especially around the ground. Moreover, the strong magnetic fields of the antenna with an extended cavity ( $h_c = 8$  mm) are confined between the lower feed loop and the ground with an average field strength of 32.6 dBA/m, whereas the value of the antenna without an extended cavity ( $h_c = 0$  mm) is 30.2 dBA/m.

To further verify the effectiveness of the proposed extended cavity structure, we analyze the average mutual



**FIGURE 8** H-field distributions according to the  $h_c$



**FIGURE 9** E-field distributions in the  $xy$ -plane ( $-20 \text{ mm} \leq x, y \leq 20 \text{ mm}, z = 8 \text{ mm}$ ). A, With extended cavity. B, Without extended cavity [Colour figure can be viewed at [wileyonlinelibrary.com](http://wileyonlinelibrary.com)]

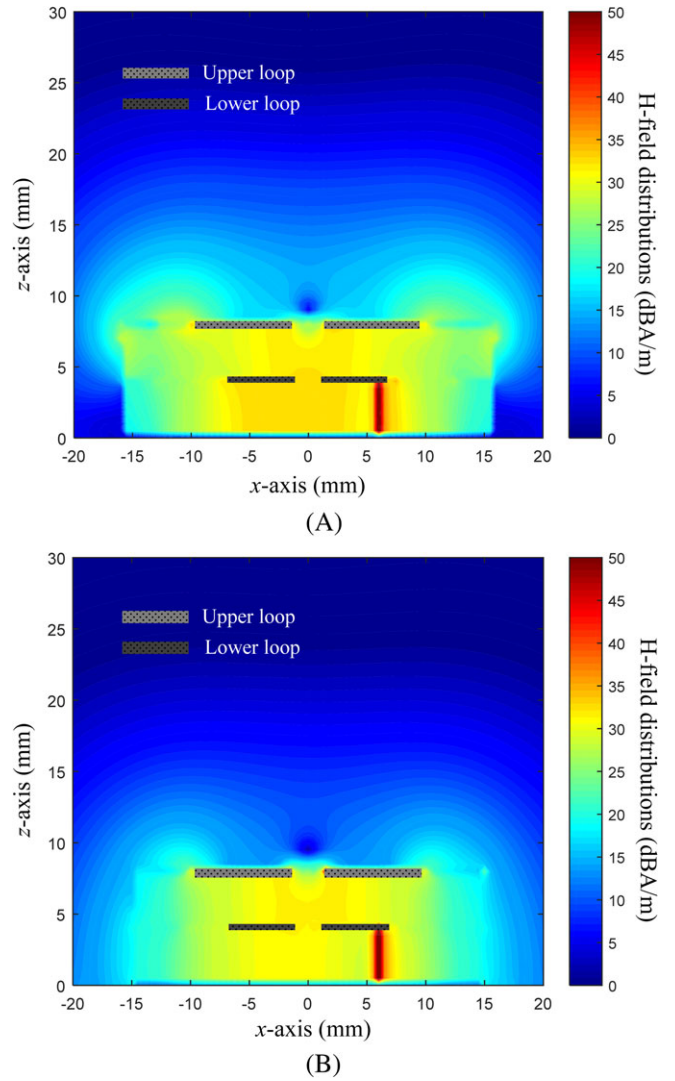


**FIGURE 10** H-field distributions ( $-20 \text{ mm} \leq x \leq 20 \text{ mm}, y = 0 \text{ mm}, 0 \text{ mm} \leq z \leq 30 \text{ mm}$ ). A, With extended cavity. B, Without extended cavity [Colour figure can be viewed at [wileyonlinelibrary.com](http://wileyonlinelibrary.com)]

coupling ( $|S_{21}|$ ,  $|S_{31}|$ , and  $|S_{41}|$ ) of the 4-element circular array according to the physical separation distance ( $d$ ) from 25 to 45 mm, as presented in Figure 11. The antennas with and without an extended cavity have identical values of  $-22 \text{ dB}$  at  $d = 45 \text{ mm}$ . The mutual coupling of the proposed antenna is slightly increased up to  $-16.4 \text{ dB}$  as the distance becomes narrower ( $d = 25 \text{ mm}$ ), whereas that of the antenna without the cavity raises to  $-11.6 \text{ dB}$ . The difference of the mutual coupling strength between array elements with and without an extended cavity is greater than  $4.5 \text{ dB}$ , indicating that the proposed extended cavity structure can improve the isolation characteristic. This improvement of the mutual coupling can avoid significant gain degradation of the array element, and the results are shown in Figure 12. In a very small array with  $d = 25 \text{ mm}$ , the gain degradation with an extended cavity is  $1.9 \text{ dB}$  which is improved by  $2.6 \text{ dB}$  compared to the antenna without the cavity. This result implies that the proposed antenna is capable of preventing the gain degradation

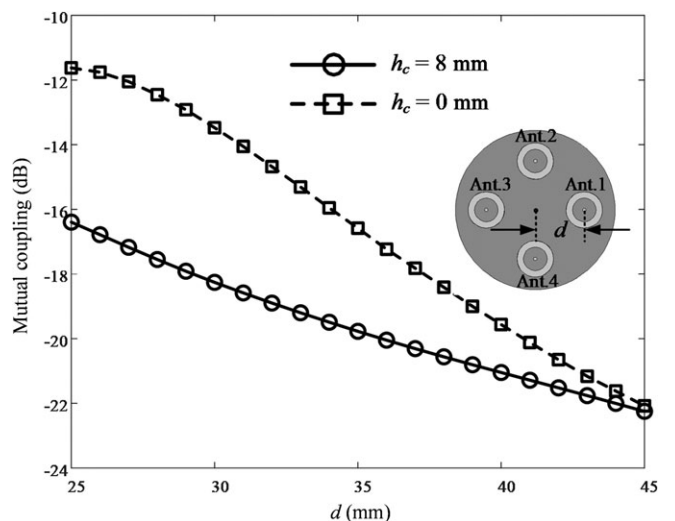


**FIGURE 11** Mutual coupling of the array according to the  $h_c$

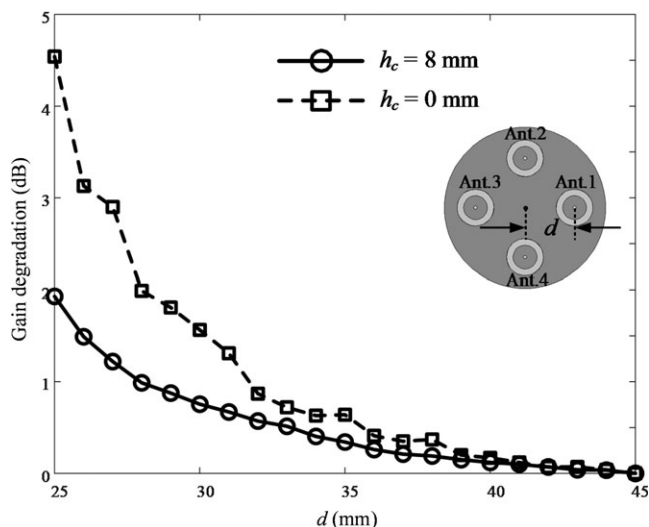


**FIGURE 12** Gain degradation of the array element according to the  $h_c$

caused by mutual coupling between adjacent array elements in very small GPS array.

## 4 | CONCLUSION

The design of an antenna element for an extremely small GPS array using dual circular loops with an extended cavity structure was proposed to reduce mutual coupling. The proposed antenna consists of a lower feed loop, an upper radiating loop, and an extended cavity structure, can avoid the gain degradation by improving the isolation characteristic with reduced leakage field strength and miniaturized aperture size. The proposed antenna had a measured bore-sight gain of 1.7 dBic at 1.575 GHz, and the gain was greater than 0 dBic from 1.53 to 1.62 GHz. We analyzed antenna characteristics including mutual coupling, bore-sight gain, near-field distributions, and resonant frequency according to the extended cavity height. The results demonstrated that the proposed extended cavity structure can avoid the significant gain degradation by reducing the mutual coupling between adjacent antenna elements in very small GPS array.

## ACKNOWLEDGMENT

This research was supported by Navcours Co., Ltd. and grant-in-aid of Hanwha Systems.

## ORCID

Gangil Byun  <https://orcid.org/0000-0001-9388-9205>

Hosung Choo  <https://orcid.org/0000-0002-8409-6964>

## REFERENCES

- [1] Cheng Y-F, Ding X, Shao W, Wang B-Z. Reduction of mutual coupling between patch antennas using a polarization-conversion isolator. *IEEE Antennas Wirel Propag Lett.* 2016;16:1257-1260.
- [2] Yang X, Liu Y, Xu Y-X, Gong S-X. Isolation enhancement in patch antenna array with fractal UC-EBG structure and cross slot. *IEEE Antennas Wirel Propag Lett.* 2017;16:2175-2178.
- [3] Hwang S, Lee B, Kim DH, Park JY. Design of S-band phased array with high isolation using broadside coupled split ring resonator. *J Electromagn Eng Sci.* 2018;18(2):108-116.
- [4] Gupta S, Mumcu G. Dual-band miniature coupled double loop GPS antenna loaded with lumped capacitors and inductive pins. *IEEE Trans Antennas Propag.* 2013;61(6):2904-2910.
- [5] Liu Z-G, Guo Y-X. Compact low-profile dual band metamaterial antenna for body centric communications. *IEEE Antennas Wirel Propag Lett.* 2014;14:863-866.
- [6] Nelaturi S, Sarma NVSN. A compact microstrip patch antenna based on metamaterials for Wi-Fi and WiMAX applications. *J Electromagn Eng Sci.* 2018;18(3):182-187.
- [7] Deshmukh AA, Ray KP. Compact broadband modified triangular microstrip antennas. *IET Microw Antennas Propag.* 2015;9(11):1205-1212.
- [8] Kang MC, Choo H, Byun G. Design of a dual-band microstrip loop antenna with frequency-insensitive reactance variations for an extremely small array. *IEEE Trans Antennas Propag.* 2017;65(6):2865-2873.
- [9] Rahmat-Samii Y, Michielssen E. *Electromagnetic Optimization by Genetic Algorithms.* Hoboken, NJ: Wiley; 1999.
- [10] Altair. FEKO. 2017. Available on-line at <https://www.feko.info>. Accessed April 21, 2017.
- [11] Ansys, Inc. Ansys Designer v2.2. 2013. Available on-line at <http://www.ansys.com>. Accessed September 11, 2015.
- [12] Balanis CA. *Advanced Engineering Electromagnetics.* 1st ed.- New York, NY: Wiley; 1989:154-168.

**How to cite this article:** Hur J, Byun G, Kim J, Kim M, Ko J, Choo H. Design of a circular dual-loop antenna for a GPS array element using an extended cavity structure. *Microw Opt Technol Lett.* 2019;61:1104-1109. <https://doi.org/10.1002/mop.31650>